Int. J. Nonlinear Anal. Appl. 13 (2022) 2, 1577–1584
ISSN: 2008-6822 (electronic)
http://dx.doi.org/10.22075/ijnaa.2021.24406.2733

An efficient framework for glioma tumor classifications and diagnosis using proposed CNN architecture

Jeevanantham V[a,*], Premkumar M[a], Ashokkumar SR[b], Anupallavi S[c], Dhamodharan S[a]

[a] *Department of ECE, SSM Institute of Engineering and Technology, Dindigul, India*
[b] *Department of ECE, Sri Eshwar College of Engineering and Technology, Coimbatore, India*
[c] *Department of ECE, VSB College of Engineering Technical Campus, Coimbatore, India*

(Communicated by Madjid Eshaghi Gordji)

Abstract

This article proposes the deep learning algorithm- Convolutional Neural Networks (CNN) for both Glioma tumor classifications and diagnosis process. This proposed CNN architecture is derived from the conventional CNN architecture to obtain the optimum classification and diagnosis accuracy. This proposed CNN architecture is derived from the conventional system for obtaining the high classification and diagnosis performance. This proposed methodology stated in this paper uses BRATS 2015 open access dataset for obtaining the brain Magnetic Resonance Image (MRI) for tumor region detection. The proposed methodology stated in this paper for tumor diagnosis achieves 97.7% of Jaccard Index (J) and 83.8% of Dice Similarity Index (DSI) and 99.025 of Diagnosis Rate (DR) using CNN algorithm..

Keywords: Glioma, tumor, deep learning algorithm, classification, diagnosis
2020 MSC: 68T05

1 Introduction

The brain is a permanent and foremost important area for storing the memory of the persons. It is the origin of all human behavior, thoughts, feelings and understanding [5], [7], [9] and [10]. It also integrates and controls relating to balance and autonomic functions in the body. The development of the uncontrolled tissue patterns in brain region causes tissue damage which leads to tumor cells. The tumor cells are rapidly developing and their boundaries are slashed with the boundaries of nearby cells in brain. The modality of the brain can be viewed in Magnetic Resonance Imaging (MRI). This paper utilizes MRI scanning modality for identifying the tumor cells in brain regions. This MRI scan produces the clear cross sectional view of the brain regions and it locates the tumor pixels. Even though many methods were developed for the last two decades for detecting the tumor pixels in brain regions, they were not able to provide high grade diagnosis factor [14] and [6]. This issue can be solved using the modified deep learning method in this article.

Hayit Greenspan et al. (2018) [3] implemented an automated segmentation algorithm to segment brain MRI images acquired under varying noise conditions using Expectation Maximization (EM) and Gaussian Mixture Model (GMM).

---

[*] Corresponding author

Email addresses: `jeevananthamrvs@gmail.com` (Jeevanantham V), `prem53kumar@gmail.com` (Premkumar M), `srashokkumar1987@gmail.com` (Ashokkumar SR), `anupallavi1991@gmail.com` (Anupallavi S), `dhamu20@gmail.com` (Dhamodharan S)

Received: July 2021 *Accepted:* September 2021

The authors claim that the algorithm was applied on different slices of T1 weighted images which were noisy and the algorithm gives superior results both visually and quantitatively. Vishnuvarthanan et al. (2018) [16] proposed bacteria foraging optimization based modified FCM algorithm, to use both optimization and clustering techniques in a single framework to improve the performance of MRI brain image segmentation. The main motivation of this work was to support non-linear factor for the present brain activation system. The drawbacks of FCM include large computation time, generation of local optimal solution, sensitive to noise to get better results. Zotin et al. (2018) [17] proposed pixel boundary method which was based on FCM algorithm. Balance Contrast Enhancement Technique (BCET) method was applied on the test source to reduce the behavior of the content noise and enhance the features of image. Then, FCM is applied to segment brain tumour region. Finally, canny edge detection is used to refine the result of FCM. Gordillo et al. (2013) [4] discussed the major types of thresholding method as the local thesholding and global thresholding. The threshold framework detected the non-linear heuristic pattern type of pixels and these pixels were grouped into different segment of regions. During the segmentation of these non-linear pixels on brain region, the overflow problem raised which degraded the tumor pixel segmentation performance. The homogeneity behavior of the segmented pixels was compared with the other region of pixels for their evaluation of the segmentation performance.

Viji et.al (2013) [15] proposed the relationship model for the pixel based texture approach for the segmentation of the pixel bounds. Here, the local texture content of the neighborhood pixels were computed and analyzed for extracting the region of pixels belonging to the other set of texture regions in the segmented image. The seed point selection procedure was now applied to the selected random pixels to improve the pixel texture behavior.

2 Proposed CNN Architecture for Glioma image classifications

Fig.1 (a) shows the Conventional CNN architecture and Fig.1 (b) shows the proposed CNN architecture. In conventional CNN architecture, the structure is designated with Convolutional, Pooling, Fully Connected Neural Network (FCNN) which are are used for the classifications of Glioma brain images as stated in Milica et al. (2020) [12]. This conventional methodology achieved 96.56% of classification accuracy. This classification accuracy is not adequate for further tumor diagnosis process. Hence, this article develops Glioma classification system through the modification of CNN structure, as illustrated in Figure 1(a) and Figure 1(b).

2.1 Data augmentation

The machine learning algorithm such as SVM and NN required huge sample sizes for Glioma case for which is used to obtain the maximum performance rate. This limitation is overcome by using the proposed CNN architecture which requires minimum number of Glioma images for training. The minimum number of Glioma brain images is increased using data augmentation method. In this paper, right shifting, left shifting and image flipping techniques are used as data augmentation methods for Glioma images for training. Totally, 424 number of samples accessed from the open access dataset as 150 brain images (normal), 220 brain images (low grade Glioma images) and 54 brain images (high grade Glioma images) [11]. All these case of brain images are data augmented before training of CNN architecture starts. Hence, the total number of brain image after data augmentation process is 1272 (424*3).

In this proposed methodology, four Convolutional layers are used as depicted in Fig. 1 (b). Each Convolutional layer consists of number of Convolutional filters which convolves the input image with its Convolutional filter kernel. The first Convolutional layer consists of 16 numbers of Convolutional filters with 5*5 kernel size. The second Convolutional layer consists of 32 numbers of Convolutional filters with 7*7 kernel size. The third and fourth Convolutional layer consists of 64 numbers of Convolutional filters with 9*9 kernel size.

The size of each Convolutional layer output is high which cannot be further processed due to high consumption of memory. In order reduce the size of the output of each Convolutional layer; pooling layer is included in the output of each Convolutional layer. In this paper, max pooling algorithm is used in all pooling layers of the proposed CNN architecture. The response from the third pooling layer is passed to FCNN.

The FCNN consist of three layers as input layer (1 number), hidden layer (5 numbers) and output layer (1 number). The input layer consists of 10 neurons and output layer consist of two neurons. Each hidden layer consists of 20 neurons. The number of neurons in each layer is fixed after testing with several iterations in order to obtain high classification accuracy [13]. Finally, morphological segmentation method as illustrated in paper is applied on the brain image to segment the pixels categorized into abnormal.

Further, the classified Glioma image can be categorized for 'Mild' or 'Severe' using the proposed CNN architecture. Fig.2 is the modified structure which helps to differentiate the different types of the using proposed CNN architecture.

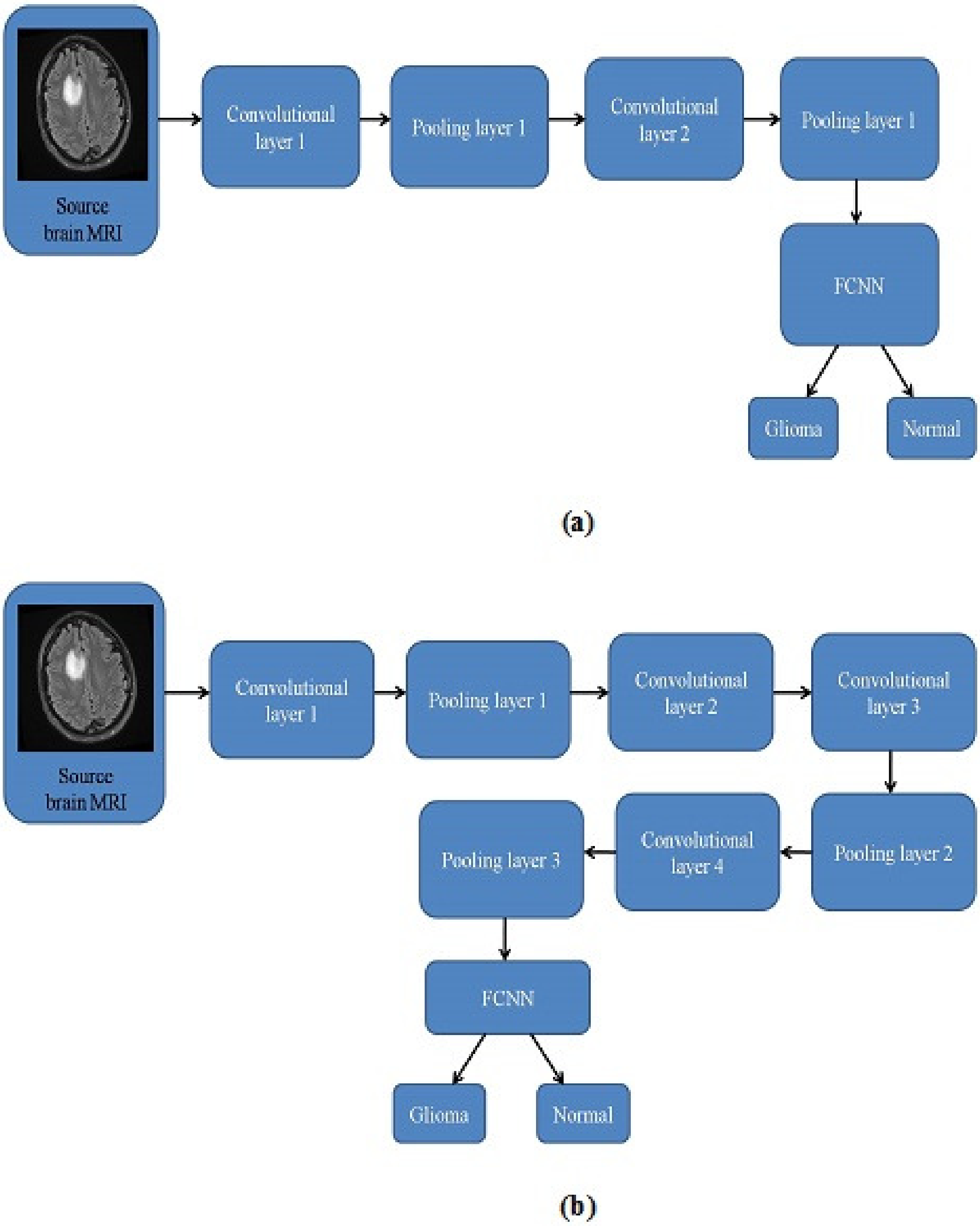

Figure 1: (a) Conventional CNN architecture (b) Modified CNN structure

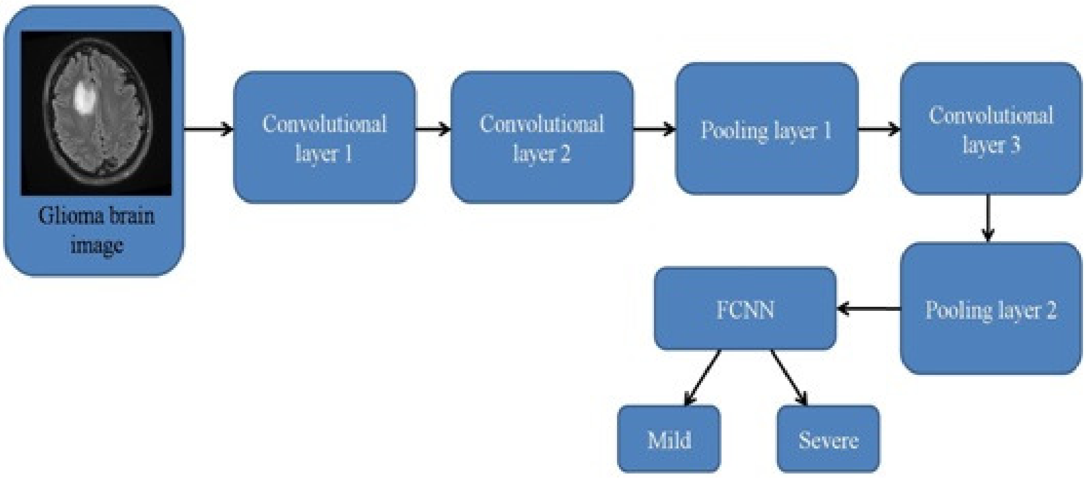

Figure 2: (a) Conventional CNN architecture (b) Modified CNN structure

The proposed CNN architecture used in this paper for Glioma tumor diagnosis process consists of three Convolutional layers and two pooling layers and one Fully Connected Neural Network (FCNN).

Each Convolutional layer consists of number of Convolutional filters which convolves the classified Glioma and the linear filter kernel. The first Convolutional layer consists of 128 numbers of Convolutional filters with 3*3 kernel size. The second Convolutional layer consists of 256 numbers of Convolutional filters with 3*3 kernel size. The third Convolutional layer consists of 512 numbers of Convolutional filters with 3*3 kernel size. The first Convolutional layer response is passed to the second Convolutional layer. The response of second Convolutional layer is passed to the first pooling layer. The response from this pooling layer is passed to the third Convolutional layer and the response of this Convolutional layer is passed to next pooling functions.

The response from the second pooling layer is passed to FCNN. The FCNN consist of three layers as input layer (1 number), hidden layer (7 numbers) and output layer (1 number). The number of neurons in each layer is decided with respect to the response size from the pooling layer.

3 Results and Discussions

The proposed methodology stated in this paper uses BRATS 2015 open access dataset for obtaining the brain MRI images for tumor region detection. This dataset consist of 150 brain MRI images with no tumor pixel, 220 high grade Glioma and 54 low grade Glioma brain images respectively. Table 1 shows the Confusion matrix for tumor and non-tumor pixel detection, which clearly correlates the tumor and non-tumor pixels with respect to positive and negative result on Glioma brain MRI images.

Table 1: Confusion matrix for tumor and non-tumor pixel detection

Test	Status of pixel	
result	Tumor pixel	Non-tumor pixel
Positive	A	B
Negative	C	D

The following performance parameters are derived from Table 1.

$$Sensitivity(S_e) = \frac{A}{A+C} \tag{3.1}$$

$$Specificity(S_p) = \frac{B}{B+D} \tag{3.2}$$

$$Accuracy(Acc) = \frac{A+B}{A+B+C+D} \tag{3.3}$$

$$PositivePredictiveValue(PPV) = \frac{A}{A+D} \tag{3.4}$$

$$NegativePredictiveValue(NPV) = \frac{B}{B+C} \tag{3.5}$$

$$FalseNegativeRate(FNR) = \frac{C}{A+C} \tag{3.6}$$

$$FalsePositiveRate(FPR) = \frac{D}{A+D} \tag{3.7}$$

$$Precision(Pr) = \frac{A}{A+B} \tag{3.8}$$

$$PositiveLikelihoodRatio(LR+) = \frac{S_e}{1-S_p} \tag{3.9}$$

$$NegativeLikelihoodRatio(LR-) = \frac{1-S_e}{S_p} \tag{3.10}$$

Table 2 and Table 3 illustrates the simulation behavior of modified CNN structure on both low and high grade Glioma images respectively.

Table 2: Performance Evaluation of proposed method on low grade Glioma images

Image Sequence	S_e (%)	S_p (%)	Acc (%)	PPV (%)	NPV (%)	FNR (%)	FPR (%)	Pr (%)	LR+ (%)	LR- (%)
1	98.1	99.2	99.5	98.7	99.2	99.2	98.8	98.9	99.5	98.8
2	98.9	98.9	99.8	98.9	98.7	99.6	98.9	98.1	99.3	98.8
3	99.9	98.9	98.9	98.7	98.8	98.9	98.8	98.9	98.6	98.9
4	99.1	98.9	99.1	98.9	98.3	99.5	97.6	98.8	98.6	98.9
5	99.1	97.9	99.3	96.9	99.8	98.9	98.9	98.1	99.7	98.1
6	99.3	99.8	99.2	98.7	99.1	99.5	99.7	98.5	98.6	98.5
7	97.8	98.9	98.9	98.9	98.7	99.5	98.3	97.8	99.5	98.8
8	99.7	98.6	99.5	98.6	98.6	98.7	98.1	97.9	99.1	98.8
9	97.9	98.7	99.8	98.4	98.6	98.7	96.9	97.6	99.9	98.1
10	99.1	98.9	98.9	98.8	99.5	99.5	98.9	99.1	99.3	97.9
Average	98.8	98.8	99.2	98.5	98.9	99.2	98.4	98.3	99.3	98.5

Table 4 analyze the ICR parameter for different cases of brain MRI images using proposed CNN methodology stated in this paper. This method classifies 149 normal brain images over 150 images, 53 LGG images over 54 images and 219 HGG images over 220 images. Hence, the ICR for normal brain images is 99.33%, the ICR for LGG images is 98.14% and ICR for HGG images is 99.54%. Therefore, the average ICR is about 99% using the modified CNN structure.

Table 5 compares the simulation responses of this modified CNN structure using ICR on different grades of brain MRI images.

The following performance evaluation parameters are used in this paper to analyze the performance of the proposed tumor diagnosis system using CNN classifier. All these parameters are computed in

$$accardIndex(J) = \frac{A}{A+C+D} \tag{3.11}$$

$$DiceSimilarityIndex(DSI) = \frac{2*A}{A+B+C+D} \tag{3.12}$$

$$DiagnosisRate(DR) = \frac{Correctlydiagnosedimages}{Totalnumberofimages} \tag{3.13}$$

Table 3: Performance Evaluation of proposed method on high grade Glioma images

Image Sequence	S_e (%)	S_p (%)	Acc (%)	PPV (%)	NPV (%)	FNR (%)	FPR (%)	Pr (%)	LR+ (%)	LR- (%)
1	98.5	98.2	99.1	98.7	97.1	99.7	98.7	98.9	98.5	98.8
2	98.6	98.8	99.4	96.8	97.7	98.1	99.5	99.8	99.6	99.1
3	98.9	98.8	99.3	99.1	99.5	98.5	96.8	98.6	98.9	98.9
4	99.7	97.9	99.1	96.3	99.8	99.7	99.8	98.8	99.6	98.3
5	97.9	98.6	99.1	99.7	99.9	99.6	98.9	98.6	99.4	99.9
6	98.8	98.8	99.6	96.9	98.9	98.9	96.9	99.6	99.6	99.1
7	97.8	98.9	99.8	99.1	99.8	98.4	99.9	98.8	99.5	98.9
8	98.5	98.1	99.7	96.8	99.9	99.7	98.9	98.9	99.7	98.8
9	98.9	98.8	99.9	99.8	97.9	98.5	97.9	97.8	99.5	99.1
10	98.9	98.8	99.7	98.1	98.9	98.9	97.1	98.3	99.8	99.5
Average	98.6	98.5	99.4	98.1	98.9	99	98.4	98.8	99.4	99.0

Table 4: ICR analysis

Methodologies	Image classification rate (ICR) (%)
Normal brain images	99.33
Low grade Glioma images	98.14
High grade Glioma images	99.54
Total	99

Where A is the correctly classified Mild case images, C is the incorrectly classified Mild case images, B is the correctly classified severe case images and D is the incorrectly classified severe case images respectively. In this paper, the proposed CNN classifier correctly classifies 88 Mild case images over 89 images, incorrectly classifies 1 Mild case image over 89 images. It also correctly classifies 120 severe case images over 89 images, incorrectly classifies 1 severe case image over 120 images, as illustrated in Table 7.

From Table 7, the proposed methodology using the modified CNN structure yields 88 mild stage images over 89 images and achieves 98.87% of DR and the proposed methodology yields 121 severe case images over 121 images and achieves 100% of DR. Hence, the average DR of the proposed diagnosis system stated in this paper is 99.43

Table 8 compares the proposed diagnosis method using CNN classifier. The proposed methodology stated in paper achieves 98.8% of J, 83.8% of DSI and 99.43% of DR.

From Table 8, the proposed tumor diagnosis system achieves high values of J and DSI when compared with conventional tumor diagnosis systems.

4 Conclusions

This paper proposes an efficient CNN architecture for both Glioma brain tumor classification and diagnosis process. This proposed CNN architecture is derived from the conventional structure for improving the high classification and diagnosis accuracy. This method classifies 149 normal brain images over 150 images, 53 LGG images over 54 images and 219 HGG images over 220 images. Hence, the ICR for normal brain images is 99.33%, the ICR for LGG images is 98.14% and ICR for HGG images is 99.54%. Therefore, the average ICR obtained through this work is about 99%. The proposed methodology using modified CNN structure for tumor diagnosis attains 97.7% of J and 83.8% of DSI and 99.025 of DR using CNN algorithm.

Table 5: Comparative Framework for brain tumor detection systems with respect to ICR

Methodologies	Total number of images	Proposed work		Abdelmajid Bousselham et al. (2019)		Parasuraman Kumar et al. (2019)	
		Number of images correctly classified	ICR (%)	Number of images correctly classified	ICR (%)	Number of images correctly classified	ICR (%)
Normal brain images	150	149	99.33	146	97.33	142	94.66
Low grade Glioma images	54	53	98.14	52	96.29	47	87.03
High grade Glioma images	220	219	99.54	215	97.72	210	95.45
Total	424	421	99	413	97.1	399	92.38

Table 6: Performance Evaluation of proposed method with conventional methods

Methodologies	Grades	S_e (%)	S_p (%)	Acc (%)
Proposed work	LGG	98.8	98.8	99.2
	HGG	98.6	98.5	99.4
Abdelmajid Bousselham et al.(2019) [1]	LGG	94.8	96.6	97.7
	HGG	93.8	96.1	97.1
Parasuraman Kumar et al. (2019) [8]	LGG	95.6	97.1	98.1
	HGG	94.8	97.5	97.9

References

[1] A. Bousselham, O. Bouattane, M. Youssfi and A. Raihani, *Towards reinforced brain tumor segmentation on MRI images based on temperature changes on pathologic area*, Int. J. Biomed. Imag. **2019** (2019), Article ID 1758948, 1–18.

[2] BRATS database, (2015). `http://braintumorsegmentation.org/`

[3] H. Greenspan, A. Ruf and J. Goldberger, *Constrained Gaussian mixture model framework for automatic segmentation of MR brain images*, IEEE Trans. Med. Imag. **25** (2006), no. 9, 1233–1245.

[4] N. Gordillo, E. Montseny and P. Sobrevilla, *State of the art survey on MRI brain tumor segmentation*, Magnetic Resonance Imag. **31** (2013), no. 8, 1426–1438.

[5] Z. Ji, Y. Xia, Q. Sun, Q. Chen and D. Feng, *Adaptive scale fuzzy local Gaussian mixture model for brain mr image segmentation*, Neurocomput. **134** (2014), no. 12, 60—69.

[6] P. John, *Brain tumor classification using wavelet and texture based neural network*, Int. J. Sci. Engin. Res. **3** (2012), no. 10, 1–7.

[7] K. Kalti and M.A. Mahjoub, *Image segmentation by Gaussian mixture models and modified FCM algorithm*, Int. Arab J. Inf. Technol. **11** (2014), no. 1, 11—18.

[8] P. Kumar and B. VijayKumar, *Brain tumor MRI segmentation and classification using ensemble classifier*, Int. J. Recent Technol. Engin. **8** (2019), no. 1S4.

[9] G.C. Lin, W.J. Wang, C.C. Kang and C.M. Wang, *Multispectral MR images segmentation based on fuzzy knowledge and modified seeded region growing*, Magnetic Resonance Imag. **30** (2012), no. 2, 230—246.

[10] I. Maiti and M. Chakraborty, *A new method for brain tumor segmentation based on watershed and edge detection algorithms in hsv colour model*, IEEE Nat. Conf. Comput. Commun. Syst. (NCCCS), 2012, pp. 1—5.

[11] N. Mathur, S. Mathur and D. Mathur, *A novel approach to improve Sobel edge detector*, Procedia Comput. Sci.

Table 7: Confusion matrix for tumor and non-tumor pixel detection

Test Result	Status of pixel Mild case (89)	 Severe case (121)
Correct	A (88)	B (121)
Incorrect	C (1)	D (0)

Table 8: Comparisons of proposed diagnosis method using CNN classifier

Methodology	J(%)	DSI (%)	DR (%)
Proposed work	98.8	83.8	99.43
Abdelmajid Bousselham et al. (2019)[1]	92.1	81.7	85.1
Parasuraman Kumar et al. (2019)[8]	90.6	80.5	82.8

93 (2016), no. 16, 431—438.

[12] P.A. Mei, C. de Carvalho Carneiro, S.J. Fraser, L.L. Min and F. Reis, *Analysis of neoplastic lesions in magnetic resonance imaging using self-organizing maps*, J. Neurol. Sci. **359** (2015), no. 1, 78-–83.

[13] K. Nimeesha and R.M. Gowda, *Brain tumour segmentation using k-means and fuzzy c-means clustering algorithm*, Int. J. Comput. Sci. Inf. Technol. Res. Excell. **3** (2013), no. 2, 60—65.

[14] T.U. Paul and S.K. Bandhyopadhyay, *Segmentation of brain tumor from brain mri images reintroducing k–means with advanced dual localization method*, Int. J. Engin. Res. Appl. **2** (2012), no. 3, 226-–231.

[15] K.A. Viji and J. JayaKumari, *Modified texture based region growing segmentation of MR brain images*, IEEE Conf. Inf. Commun. Technol. (ICT), 2013, pp. 691—695.

[16] A. Vishnuvarthanan, M.P. Rajasekaran, V. Govindaraj, Y. Zhang and A. Thiyagarajan, *Development of a combinational framework to concurrently perform tissue segmentation and tumor identification in T1-w, T2-w, Flair and MPR type magnetic resonance brain images*, Expert Syst. Appl. **95** (2018), no. 15, 280–311.

[17] A. Zotin, K. Simonov, M. Kurako, Y. Hamad and S. Kirillova, *Edge detection in mri brain tumor images based on fuzzy c-means clustering*, Procedia Comput. Sci. **126** (2018), 1261—1270.